A Portable Device for miRNAs Detection Based on a Gold-nanoparticle Ratiometric Colorimetric Strategy

Adrián Sánchez Visedo, Jorge Losada Matías, Ana Soldado Cabezuelo, José Manuel Costa Fernández, María Teresa Fernández Argüelles, Marta Valledor Llopis, Juan Carlos Campo Rodríguez, *Member, IEEE*, Francisco Ferrero Martín, *Senior Member, IEEE*

***Abstract*— MicroRNAs (miRNAs) have recently emerged as a new class of biomarkers for disease diagnosis and play vital roles in physiological and pathological processes. Here, a novel fiber-optic prototype that allows synchronized optical transmittance measurements at different wavelengths has been designed and fabricated for selective and sensitive miRNAs detection based on a ratiometric colorimetric strategy. The proposed measurement method automatically adjusts the output light power through the LEDs, minimizing eventual differences in brightness and potential losses through the optical fiber without the need expensive optical components. The prototype has been validated for the detection of miRNAs identified as biomarkers of bovine mastitis in dairy cattle. Observation of the color changes from red to blue of the AuNP solution, and therefore on the transmittance signal, caused by miRNA-induced gold nanoparticles aggregation has been used for rapid detection of such genetic biomarker. The equipment designed and constructed is portable, being the main parameters of the measurement managed with a smartphone, and it could be potentially employed with any other biosensor whose detection strategy is based on changes in the distance between gold nanoparticles.**

***Index Terms*—gold nanoparticles, mastitis, microRNA, optical biosensor, ratiometric methods, smartphone interface.**

I. INTRODUCTION

CLEARLY real-time and in-situ monitoring of biomolecules that provide useful information before the food reaches the food chain, or to carry out an early detection of a certain disease constitutes a demand in agro-food industry. In this context, micro RNAs (miRNA) are considered as crucial regulators of gene expression and promising candidates for biomarkers of food quality [1], [2]. They contain between 19 and 25 nucleotides that suppress the expression of protein-coding genes.

Financial support from Principado de Asturias (Spain) through the project FC-GRUPIN-IDI/2021/000081, from the Ministry of Science and Innovation (Spain) through the projects Ref. PID2019-109698GB-I00 and PID2020-117282RB-I00), from the Fundación Española para la Ciencia y la Tecnología through the project MCIU-20-FCT-PRECIPITA, and from Banco Santander and University of Oviedo through the project PAPI-19-PF-22, is gratefully acknowledged.

The authors are with the Department of Electrical and Electronic Engineering, University of Oviedo, 33204, Spain (e-mail: ferrero@uniovi.es), and the Department of Physical and Analytical Chemistry University of Oviedo, 33006, Spain (e-mail: fernandezteresa@uniovi.es).

miRNAs are key players in several biological processes, such as cellular proliferation and differentiation, apoptosis and in numerous immunological and inflammatory disorders. Thus quantitative and rapid detection of a specific miRNAs can provide critical information for diagnosis of different pathologies [3]–[7].

The reference method to measure miRNA is PCR (Polymerase Chain Reaction) analysis. However, despite the advantageous features such as sensitivity and selectivity, PCR is an expensive and time-consuming process where the presence of highly skilled personnel for both, sample analysis and data treatment, is needed. Recent methods for miRNA detection have exploited the advantageous features of nanomaterials, including gold, silver or copper nanoparticles, quantum dots or magnetic nanoparticles. To improve the sensitivity of the detection of miRNA, many approaches have been aimed to combine the use of nanomaterials with nucleic acid amplification techniques, including rolling circle amplification (RCA), duplex-specific nuclease (DSN)-based amplification, loop-mediated isothermal amplification (LAMP), exponential amplification reaction (EXPAR) and strand-displacement amplification (SDA). Despite these methods achieve a very good sensitivity, with limits of detection between picomolar to femtomolar concentration, they typically require longer incubation times for the amplification step. An overview with detailed information on this topic can be found in recently published reviews [8], [9]. Therefore, nowadays a great effort is being pursued towards the development of alternative measurement systems to carry out a fast, easy to use, low-cost and in-situ detection of miRNA.

To meet these challenges, parallel development in electronic instrumentation is essential. Portability is highly appreciated, together with the use of friendly interfaces that simplify the measurement process [10]. Moreover, handling small and compact devices that allow the use of smartphones or tablets as user interfaces saves time, and reduces the cost of development. Additionally, the touch screen technology present in smartphones allows configuring the measurements easily and intuitively by non-qualified personnel [11], [12].

There are many sensing devices described for bioanalytical applications based on measurements of spectroscopical changes. In this sense, when looking for a simple device, a colour changes specifically produced in presence of the analyte presents the important advantage of allowing a very simple detection only with the naked eye. However, this strategy also has several limitations. Probably,

the most important limitation is the bias derived from the perception of the colour by different analysts, giving rise to false positive or false negative results.

The light intensity is the simplest solution for most optical fiber sensors and can be used for all cases. However, the use of light intensity introduces some problems in measurement processes because the light intensity is also sensible to other variables. This fact causes both perturbation and noise and reduces the accuracy of measurement. That is why ratiometric measurements are preferred to rather than measure intensity. The objective of ratiometric techniques is to make the result independent from the main sources of error. This independence is achieved by quantifying at least two parameters proportional to the disturbance which needs to be eliminated. This perturbation will be canceled out, when it appears both in the numerator and in the denominator of the quotient that defines the ratiometric expression. The existing ratiometric techniques can be classified into two general groups named "wavelength-ratiometric methods" [13], [14] and "dynamic-ratiometric methods" [15, 16]. In both cases the results are a ratio of intensities. The difference is based on the way used to separate the two signals required to implement the ratiometric expression [17]". The proposed work belongs to the "wavelength-ratiometric methods" group.

Alternatively, in this work a new ratiometric scheme is proposed, based on an electronic automated process devoted to cancel the main fluctuations in the excitation light source, as well as to cancel variations in the optical path.

The system here developed is based on the measurement of changes in the optical properties detected after a target-induced aggregation of gold nanoparticles (AuNPs). It is well known that the localized surface plasmon resonance (SPR) band of AuNPs depends, among others, on the distance between the nanoparticles [18], [19]. The AuNP optical extinction has a maximum at the SPR frequency that can be easily measured through absorption spectroscopy. Hence, when AuNPs are far from each other the SPR peak is located at a certain wavelength, whereas when AuNPs are in close distance the SPR is shifted towards higher wavelengths. This feature has been exploited for the detection of many different types of analytes, such as proteins, DNA, RNA, etc. Specifically, this work has been evaluated for the detection of a model miRNA, which has been carried out through the controlled aggregation of AuNPs in the presence of the sequence of interest [20].

miR146a has been selected as model biomarker to validate the proposed measurement method with a practical application. miR146a is overexpressed in milk, tissue and serum samples of cows with bovine mastitis, an inflammation of the mammary gland caused by a bacterial infection, which is a highly prevalent and costly disease of dairy cattle [21], [22]. As a result, there is a great demand for robust and rapid assay platforms to enable accurate and efficient detection of low levels of such miRNAs in bovine milk.

Here AuNPs were synthesized, and surface modified with two different thiolated DNA sequences that are complementary to the target miR146a. The presence of the target in the medium brings the nanoparticles in proximity, and the colour observed changes from red to purple. A novel fiber-optic prototype that allows synchronized optical transmittance measurements at different wavelengths has been designed and fabricated for robust miR146a detection based on the AuNPs-based colorimetric strategy. This paper is an extended version of a previously published proceedings paper [23].

II. Proposed Measurement Method

The absorption spectra of RNA-modified AuNPs in absence of the target analyte, and in presence of 40 nM miR146a have been recorded with a commercial spectrophotometer. Figure 1 shows the spectra of AuNPs that are shifting in the wavelength domain when the concentration of miR146a is changing. I_0 is the intensity of the incident radiation and I is the intensity of the transmitted radiation. As can be observed in Fig. 1, the presence of the analyte generates a decrease of the recorded transmitted light at 525 nm, along with a red shift of the SPR peak from 525 nm to 540 nm. Conversely, presence of the target gives a rise to an increase on the transmitted light at higher wavelengths (645 nm). The selection of the second wavelength was carried out considering that a good change in the spectra is observed for different concentrations of the target. First, the blank and the sample are radiated at 525 nm using two green LEDs. After that, the blank and the sample are radiated at 625 nm using two red LEDs. At those wavelengths (525 nm and 645 nm) the transmitted light presents a greater difference between the sample of 10.0 nM and the blank of 0.0 nM miRNA concentration. This unique behavior is the key point on which the proposed measurement method is based. Fig. 1 also shows a picture of the sample holder containing AuNPs in presence and absence of target. When the distance between AuNPs is substantially larger than the average AuNP diameter the observed color is red. However, when the interparticle distance is less than the average AuNP diameter, the observed color changes to purple due to the AU surface plasmon resonance [24].

The difference between the colors (pink/reddish for the blank and purple in presence of target) can be easily observed using naked eye. However, quantification of the target based on color change is not possible, and a reduced sensitivity is achieved, using naked eye detection.

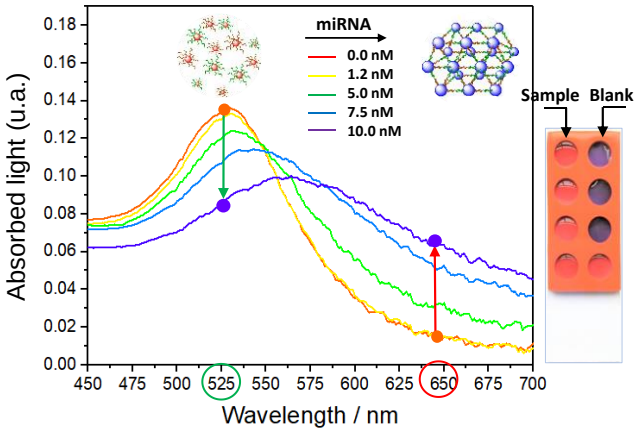

Fig. 1. Scheme of the miR146a detection based on target induced AuNPs aggregation, and the spectra of AuNPs that are shifting in the wavelength domain when the concentration

of miR146a is changing.

Changes in the presence of miRNA are noticeable at 525 and 645 nm. On the right side, an image of the sample holder containing AuNPs in the presence and the absence of target can be observed, with the subsequent change of colour.

Taking advantage of the aforementioned changes produced in the absorption spectra, the here-proposed method consists in measuring the transmittance changes (increase and decrease) at the selected wavelengths (525 and 645 nm, respectively) within presence and absence of miRNA. It should be noted that the designed prototype also allows simultaneous measurement of the blank, that is carried out when measuring different concentrations of miRNA, both at 525 and 645 nm. Once the optical signals reaching the photodetector have been processed, the transmittance signal is calculated for the chosen wavelengths of the spectra to perform the different data treatments.

The design of the detection assay was carried out using 20 nm AuNPs to generate changes in the SPR peak in presence of the analyte as reported in a previous work [20]. Hence, citrate stabilized AuNPs were synthesized following the Turkevich method [25]. The batch of AuNPs was divided in two portions, and the surface of the nanoparticles was modified using two different thiolated RNA oligonucleotides, one for each portion of AuNPs. The sequences of the thiolated RNA were designed to be complementary to the sequence of the analyte. The target is miR146a, a short RNA sequence that contains 24 RNA bases. Hence, the presence of miR146a in the medium leads to a hybridization of the complementary oligomers, bringing the AuNPs in proximity. This fact produces a modification in the SPR peak, and a color change from red to purple/black takes place. Once the miRNA and AuNPs have hybridized during a step that takes place for 20 minutes at 60ºC, the detection of the miRNA takes place. For this purpose, a blank containing all the reagents except the target, and the standard containing all the reagents are placed onto the sample holder, introduced in the developed prototype, and the measurement takes place within 2-3 seconds. Results are displayed in the smartphone application once the measurement is performed.

III. Measurement Light System

Fig. 2 shows the basic block diagram for measuring light transmission signals. The signal from the LEDs is a square signal, modulated at a certain frequency (F_{MOD}), which will be demodulated at the output of the photodiode. Then, the signal is analog-to-digital converted (ADC) and received by the microcontroller (µC). The output signal of the photodiode (PD) is a very low current, so it is amplified through a transimpedance amplifier (AMP) before entering the demodulator stage (DEM). The reference frequency from the microcontroller is used to modulate the LEDs and to demodulate the signal from the photodiode.

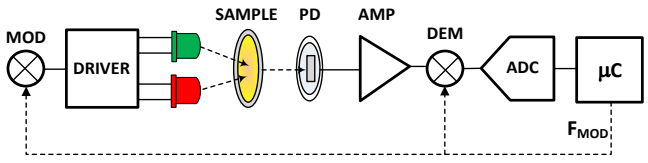

Fig. 2. Basic block diagram for measuring light transmission signals.

The measurement system can be divided into two parts: optical and electronic subsystems, as shown in Fig. 3. In the optical subsystem the sample holder allows for measuring four samples and four blanks. The optical signal provided by the blank was employed to estimate the transmittance of the sample. With the developed prototype, the LEDs employed emit certain intensity, and we measure the intensity that reaches the detector after interaction with the sample, to obtain the transmittance, which is the fraction of incident light that is transmitted.

The hardware system and the smartphone application [23] were designed to measure the blank and the sample simultaneously. To fulfil this aim, the sample holder has two columns: the one on the left employed to place the sample and the one on the right for the blank, as can be seen in Fig. 1.

The sample holder can be moved manually to measure the desired wells. It has been designed by using magnets to ensure that wells and optical fibers are properly aligned when moving from one sample holder to another. Therefore, the measurement is always performed at the center of the well, to achieve a good repeatability.

Since the wavelengths chosen for the measurements are 525 nm and 645 nm, LEDs with emission centered at those wavelengths were selected. As shown in Fig. 3, four LEDs are used, allowing measurement of two wells simultaneously, corresponding to sample and blank, respectively. For each well, a 525 nm LED (displayed in green in Fig. 3) and a 645 nm LED (displayed in red) are used.

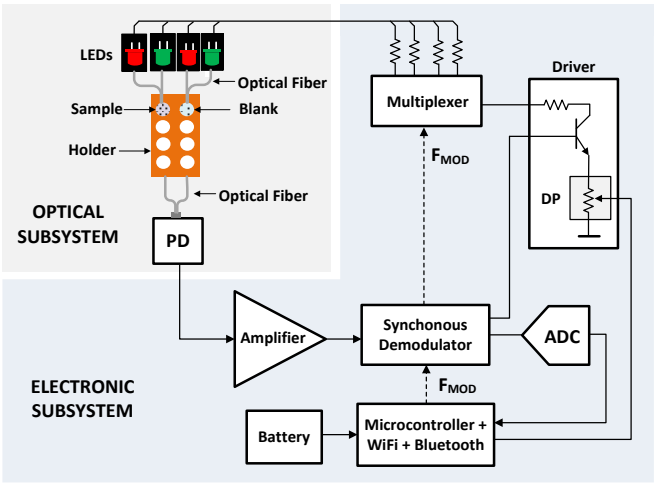

Fig. 3. Block diagram of the proposed measurement system. LEDs (Thorlabs, LED525L9 and LED645L), PD=Photodiode (Hamamatsu S1226), Multiplexer (ADG704), ADC=Analog-to-Digital Converter (Texas Instruments AD8317), Microcontroller (Expressive Systems, ESP32), Synchronous demodulator (Analog Devices, AD630), DP=Digital Potentiometer (Analog Devices, AD8400), Operational amplifier (Analog Devices, OPA124), Optical Fiber (Thorlabs FP1000ERT, core 1 mm, cladding 1035 mm), Lithium polymer battery (3.7 V, 1800 mAh, LP603870).

To ensure that the same amount of optical power from the LEDs is correctly coupled into the optical fiber firstly two precision current sources were designed according with the specific output power-current characteristic of each LED (Figure 4). The output power was set at 5 mW. Finally, the optical power was measured at the end of the fiber optic using an optical power meter from Sun Telecom (SUN-OPM200-BC). On the other hand, the ageing of the components and other factors can affect the precision of the current through the LEDs and so the output optical power. That is why the ratiometric techniques play an important role.

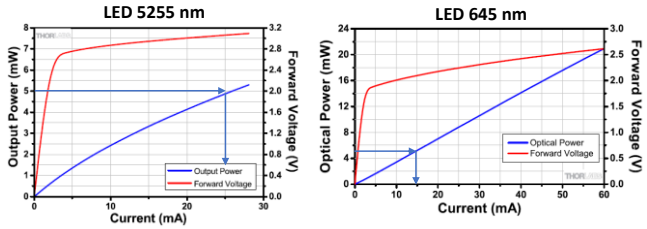

Fig. 4. Output power-current characteristics of the LEDs used.

The light emitted by the LEDs is guided through an optical fiber to both wells, and the light transmitted from the sample is then conducted to a photodiode using optical fibers, part number FP1000ERT from Thorlabs. To couple LED light into the fibers no lenses were used. The SMA connectors and the LEDs are joined in an enclosure made in the lab. The signal from the photodiodes is amplified and sent to the synchronous demodulator where it is demodulated. The modulated and demodulated processes are carried out at the reference frequency generated by the microcontroller. Finally, the signal is analog-to-digital converted to be processed by the microcontroller to calculate the transmittance ratio.

The modulation frequency of the LED light was 1 kHz. This frequency must not be so high as to compromise the dynamic limitations of the rest of the components of the system or so low to be confused with signals from artificial lighting or other sources.

The key points related to the design of the measurement system are the following: (i) The microcontroller board (LOLIN D32) is specific for the Internet of things (IoT) applications, which manages the smartphone application through Bluetooth technology. (ii) The synchronous demodulator (ADA2200), also known as lock-in amplifier, enables accurate measurement of small AC signals in the presence of noise interference orders of magnitude greater than the signal amplitude. This circuit enables a simple low-pass filter to remove most of the remaining undesired noise components [27]. (iii) The multiplexer (ADG704) employed separates the four optical excitation signals in different time. Therefore, no selective optical filtering is necessary to separate the optical signals. (iv) Automated calibration adjusts the current through the LEDs using digital potentiometers (AD8400), so that the differences in brightness of the LEDs and the losses in the optical fiber are cancelled. (v) The firmware of the microcontroller consists of the following main steps: 1) to configure the synchronous demodulator, 2) to read the ADC; 3) to average the measurements; 4) to calculate the differences. (vi) The photodiode output current is amplified by using a transimpedance amplifier (TIA) designed by means of an extremely low input bias current and low noise precision operational amplifier (OPA124). To design the photodiode amplifier special design techniques must be considered [28].

Fig. 5 shows different view sides of the developed prototype, where it can be observed how the optical fibers are connected to the sample holder, which has been designed and built in our laboratory using a 3D printer. The sample holder allows to place a conventional microscope slide with an adhesive silicone isolator to create 8 wells.

This enables the measurements of four samples and four blanks with the same slide to be carried out. Fig. 5B shows how the position of the sample holder can be moved to perform the measurement of multiple samples. Additionally, it is worth to mention that other mechanical structures have been designed to support different types of sample holders, such as traditional UV-Vis cuvettes. This enables different volumes of sample to be measured if needed, giving great versatility to the equipment to adapt to the demands of the end-user.

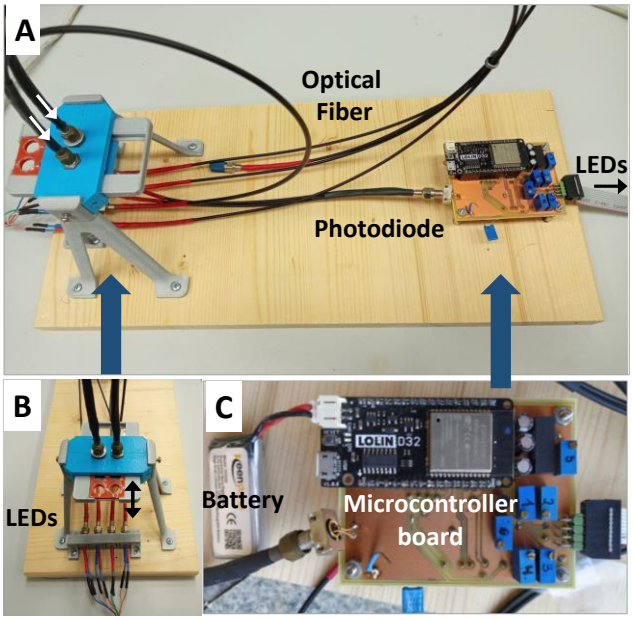

Fig. 5. Images of the developed measurement system. A: General view of the prototype; B: Fiber optics system; C: Printed circuit board of the electronic subsystem.

Autonomy is essential for a portable device. Therefore, the system has been provided with a 3.7 V, 1800 mAh lithium polymer battery employed to power the entire system. The system can be powered by micro-USB (which also charges the battery), giving it a range of several hours. The autonomy of the equipment is subject to its use. The highest consumption occurs during measurement, and it hardly consumes energy at sleep mode. The equipment communicates with a mobile phone via Bluetooth technology. If this is not possible, a low consumption mode is activated, and the battery starts to recharge. A software application based on Java language has been developed using Android Studio. The aim is to manage the automatic calibration,

the type of measurement and to show results.

A smartphone system control application has been developed and implemented in the prototype to ensure a user-friendly device. The smartphone application, that was named Nano Sensor (NS), makes an automatic calibration of the optical power of each LED before measurement. Data is stored and processed in a database that runs on the user's mobile phone, therefore the measured data is private for each user, although it can be sent in CSV format from the application itself. Calibration data can also be graphically represented, and miRNA concentration value is automatically obtained and showed in the screen. More details can be found in [23].

IV. Data Analysis

As shown in Fig. 1, target-induced aggregation of the functionalized AuNPs produces a change in the color that can be quantified by measuring the transmittance signal. Moreover, it was observed that such change in the transmission spectra of the AuNPs is selective and proportional to the miR146a concentration. The transmittance (*T*), defined as the fraction of incident light which is transmitted (*I*/*I*o), has been calculated for both wavelengths. For this purpose, the ratio of the intensity measured for the sample divided by the intensity measured for the blank was calculated at different target concentrations.

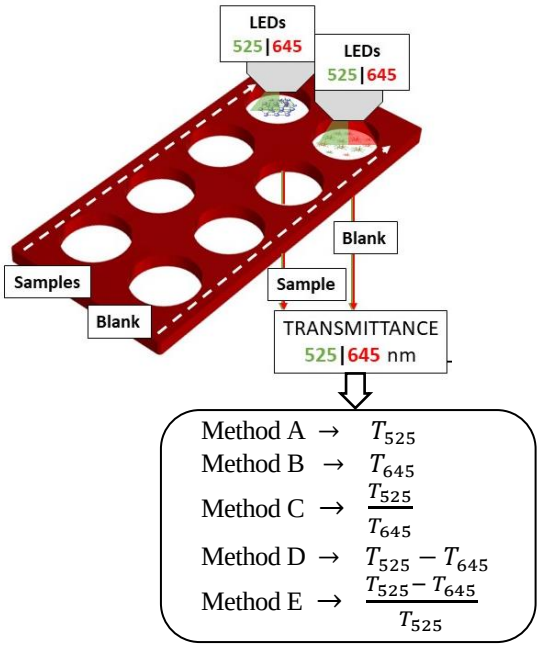

Fig. 6. Scheme of sample measurements and signal data treatment.

Methods A and B are based on the changes produced on the transmittances at 525 (T_{525}) and 645 (T_{645}) nm, respectively. The mathematical expressions of T_{525} and the T_{645} are defined as (1):

$$T_{525} = \frac{I_{sample\,(525)}}{I_{blank\,(525)}}; \qquad T_{645} = \frac{I_{sample\,(645)}}{I_{blank\,(645)}} \qquad (1)$$

Then, different mathematical treatments can be carried out for methods C, D and E, using the equations shown in Fig. 6. The different data treatments (A to E) were evaluated for increasing concentrations of miRNA as summarized in Fig. 6, and the obtained results were critically compared. For methods A and B, the transmittance signal was obtained at 525 nm and 645 nm, respectively, and plotted against target concentration.

This is the simplest data treatment approach, just based on changes on the transmittance signal of the AuNPs at a given wavelength. It can be expected that if we consider the changes produced at two wavelengths at the same time, the change on the signal would be increased in presence of the target. Hence, Methods C to E consider the change on the signal at 525 nm together with the change of the signal at 645 nm in presence of the analyte. For this purpose, different ratiometric data treatments were also evaluated based on the signals measured at 525 and 645 nm, respectively. In Method C, the ratio between the transmittance at 525 nm divided by the transmittance at 545 nm is plotted against the target concentration. In Method D, the difference between the transmittance at 525 minus the transmittance at 645 nm is calculated and plotted against the target concentration.

Finally, in Method E the difference between sample transmittances at 525 and 645 nm, divided by the transmittance at 645 nm is plotted against target concentration. Performance of the different data treatments for sensing of miRNAs are critically compared in the next section. The instrumental fiber-optic prototype constructed, capable to perform synchronized optical transmittance measurements at different wavelengths, has been evaluated for miRNAs detection based on the different ratiometric strategies proposed. For such purpose, the assay for detection of miR146a was carried out by mixing two sets of AuNPs surface modified with RNA strands that are partially complementary to the sequence of the target, with different concentrations of the analyte. After a 20-minute hybridization at 50ºC, absence of target does not produce any change in the optical properties of the AuNPs. However, the presence of miR146a generates an approximation of the AuNPs due to the hybridization of the complementary RNA bases. This distance shortening produces changes in the optical properties of the AuNPs, as displayed in Fig. 1, giving rise to a change of the observed color from red to dark purple.

The developed prototype has been designed to simultaneously measurement of the optical signal of the sample and the blank at two wavelengths, 525 and 645 nm respectively. Such wavelengths were chosen because they suffer an important change depending on the distance between the AuNPs. As it can be observed in Fig. 1, when the AuNPs become close to each other, a decrease in the absorption signal occurs at 525 nm, whereas an increase in the absorption takes place at higher wavelengths (e.g., 645 nm).

Solutions containing the AuNPs with and without miRNA are deposited in the wells for sample and blank respectively, created using a microscope glass slide and an eight well silicone adhesive barriers. The sample holder can be moved easily back and forward to measure at different positions. Moreover, magnets were incorporated to the sample stage to ensure that after moving the microscope glass slide, the wells are optimally aligned with

the optical fibers. Hence, with the same microscope slide, four different samples can be measured consecutively.

Transmittances of the blank and of the sample are registered at 525 and 645 nm. As can be seen in Fig. 6 different mathematical treatments of such measured transmittance signals were carried out to correlate them with different miRNA concentrations. Fig. 7 shows the graphs of the experimental transmittances as a function of the target concentration for the five methods. The response obtained for different concentrations of miR146a, applying calculations proposed in methods A to E, was evaluated in triplicate from 0 nM up to 40 nM. A summary of the results obtained for each proposed method are shown in Table I, including the calculated detection limit, quantification limit, range and the coefficient of determination (R^2) estimated for a sample containing a known concentration of the target.

Methods A and B, just based on the transmittance measured at a single wavelength: 525 nm and 645 nm respectively. Results have shown a good detection limit and sensitivity. This last term is defined by the International Union of Pure and Applied Chemistry as the slope of the calibration curve [29], but a poor R^2. These methods based on the measurement of the transmittance at 525 or 645 nm could be mainly employed for screening purposes.

As aforementioned, since an opposite change in the transmission signal is observed in presence of the target at two wavelengths, taking into account both changes might give rise to a greater change of the signal in presence of the analyte. As expected, considering the signals obtained at both wavelengths together has provided much better results in terms of sensitivity, linear range, and accuracy. Thus, three different approaches have been investigated: method C uses and analytical signal de ratio between the transmission at 525 and 645 nm. Method D makes use of the difference in the transmittance at 525 nm (which increases with the miRNA concentration) and 645 nm (in which an increase in the miRNA result in a decrease in the transmittance). Thus, the idea is to amplify the observed change in the total transmission signal measured. Finally, method E is a ratiometric method consisting in the ratio between the difference in signals used in method D and the transmission signal measured at 525 nm. The range obtained for methods C, D and E goes up also to 40 nM, with better R^2, although the detection and quantification limits are worse than methods A and B.

Besides the better sensitivity achieved with all those methods when compared to the visual readout (just based on the observation of the color change, where the limit of detection is on the order of the 10 nM), the method here proposed also allows the quantification of miRNA in a wide linear range, something that is not possible when performing visual detection, where a positive/negative response above a certain cut-off concentration is provided.

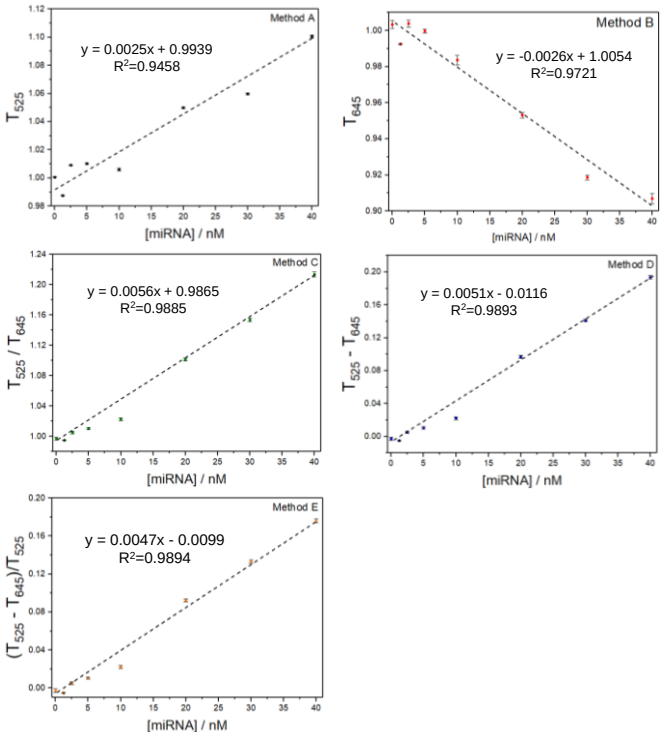

Fig. 7. Representation of the different data treatments evaluated against the concentration of miRNA (n=3).

TABLE I
FIGURES OF MERIT OBTAINED FOR THE DIFFERENT PROPOSED METHODS

Method	Detection Limit (nM)	Quantification Limit (nM)	Range (nM)	R^2
A	0.38	1.3	0.38 – 40	0.9458
B	2.5	8.3	2.5 – 40	0.9721
C	0.98	3.3	0.98 – 40	0.9885
D	1.1	3.6	1.1 – 40	0.9893
E	1.2	3.9	1.2 – 40	0.9894

The detection limit has been calculated as the concentration of analyte that produces an analytical signal three times the standard deviation of 10 measurements of a blank. The quantification limit has been calculated as the concentration of analyte that produces an analytical signal ten times the standard deviation of 10 measurements of a blank. The relative error has been estimated for the highest concentration of miRNA of the linear range for each method, as the spiked miRNA concentration minus the found miRNA concentration divided by the spiked miRNA concentration (all multiplied by 100 to provide the relative error as a percentage).

V. Discussion and Conclusion

In the last years, a growing number of publications related to the detection of miRNA using ratiometric methods can be found in the literature. A considerable number of publications rely on fluorescent techniques, followed by electrochemical and SERS detection techniques. Due to the high sensitivity accomplished with these techniques, when compared with absorption spectroscopy, a high percentage of those works

also include an amplification strategy, giving rise to methodologies that achieve low detection limits on the miRNA detection in the order between aM and fM concentration. A summary of comparisons of different miRNA ratiometric detection strategies can be found in a recent publication [30].

To the best of our knowledge, this is the first ratiometric-based method using the spectrophotometric detection technique. The detection strategy is based on the measurement of changes produced on the optical properties of functionalized AuNPs in presence of the target analyte. The measurement setup is based on a ratiometric method, which has endowed the equipment with the required robustness to work in a non-controlled environment as required for in situ applications.

Five different data treatment methods have been proposed and their analytical performance for miRNA quantification has been critically evaluated.

On the other hand, the developed prototype is competitive in offing a quick response, providing quantitative information about the presence of a certain miRNA in the sample, it is portable and can be used by non-qualified personnel thanks to the smartphone application. By last, it is worth mentioning that its IoT microprocessor makes possible to carry out remote management of the obtained data, allowing further data treatment if needed for other applications as well as to share or store data in the cloud.

Applied to dairy production, it can inform about whether the cow has mastitis, even sub-clinical, with no visible symptoms. This information is very useful for the farmer since it is reliable and allows the digital management of the already sick animals and those most susceptible to finally somatise the disease.

The prototype has been developed to provide a quantitative measurement of the concentration of miRNA146a in raw milk samples due to its correlation to bovine mastitis. However, an extraction step of the miR146a from raw milk to ultrapure water must be performed prior to the measurement. Therefore, because the complex sample matrix is removed during the extraction of the genetic material, it is expected that any other types of samples, such as urine, blood, serum, etc. can be analyzed following the same methodological procedure.

Regarding the potential detection of any other genetic target, the prototype can be used to detect other sequences of miRNA, DNA and RNA, by just changing the sequences employed to decorate the surface of the AuNPs. In this context, due to the eventual limitation in the length of the genetic target, the most difficult scenario (because of possible cross-reactivity limitations) is the detection of short single-stranded miRNA molecules. Detection of either DNA or RNA sequences of several tents of nucleotides have been performed in our laboratories, and successfully reported in the literature.

It is worth to mention that there are many biosensors described in the literature based on the use of AuNPs for the detection of analytes of different nature, including pathogens, antigens, metabolites, genetic targets, etc. Hence, despite the prototype has been validated for the detection of miR146a using a conventional laboratory spectrophotometer, a biomarker of mastitis in cows, it can be easily adapted to the detection of virtually any other genetic sequence, as well as to the detection of other analytes when the biosensor is based on changes on the distance between AuNPs. Therefore, this prototype can be considered as a general measurement platform for different analytical applications based on the use of AuNPs. The developed prototype can be considered not only as user friendly but also cost affordable device. In fact, an estimation of the total cost of all the optoelectronic components was below $100.

APPENDIX

All reagents were of analytical grade and used without any further purification unless otherwise mentioned. Hydrogen Tetrachloroaurate Trihydrate ($HAuCl_4 \cdot 3H_2O$), Sodium citrate tribasic dihydrate ($Na_3C_6H_5O_7 \cdot 2H_2O$), Magnesium Chloride Hexahydrate ($MgCl_2 \cdot 6H_2O$), Trizma® Hydrochloride ($NH_2C(CH_2OH)_3 \cdot HCl$) and Potassium Chloride (KCl) were purchased from Sigma-Aldrich (St. Louis, USA; www.sigmaaldrich.com). Thiolated Polyethylene Glycol (mPEG-SH1000) from Laysan Bio, Inc. (Huntsville, USA; www.laysanbio.com). The thiolated DNA strands employed to functionalize the AuNPs surface were: (Probe-1) 5'-SH-A AAA AAA AAA AUU CAG UUC UCA-3′, (Probe-2) 5'-ACA ACC UAU GGA AAA AAA AAA A-HS-3′and were obtained from Integrated DNA Technologies (Iowa, United States; www.idtdna.com). The micro-RNA selected as mastitis biomarker was the miR146a: 5'-UGA GAA CUG AAU UCC AUA GGU UGU-3′, from Integrated DNA Technologies. Milk samples were obtained from the Department of Animal Nutrition, Grassland and Forages, Regional Institute for Research and Agro-Food Development (SERIDA, Asturias, Spain). RNA extraction was performed using QIAzol Lysis Reagent from QIAGEN (USA; www.qiagen.com) and mirVana microRNA Isolation Kit and Phosphate-Buffered Saline (PBS) from Thermo Fisher Scientific (USA; www.thermofisher.com).

REFERENCES

[1] M. Díaz-González, A. de la Escosura-Muñiz, M. T. Fernandez-Argüelles, F. J. García Alonso, and J. M. Costa-Fernandez, "Quantum Dot Bioconjugates for Diagnostic Applications," *Top. Curr. Chem.*, vol. 378, no. 2, p. 35, Apr. 2020.

[2] M. Laura, M. Zougagh, M. Valcárcel, and Á. Ríos, "Analytical Nanoscience and Nanotechnology : Where we are and where we are heading ☆," *Talanta*, vol. 177, no. August 2017, pp. 104–121, 2018.

[3] B. P. Lewis, C. B. Burge, and D. P. Bartel, "Conserved seed pairing, often flanked by adenosines, indicates that thousands of human genes are microRNA targets," *Cell*, vol. 120, no. 1, pp. 15–20, 2005.

[4] S. Deng, J. Lang, G. Coukos, and L. Zhang, "Expression profile of microRNA in epithelial cancer: diagnosis, classification and prediction," *Expert Opin. Med. Diagn.*, vol. 3, no. 1, pp. 25–36, 2009.

[5] R. Kulshreshtha, R. V. Davuluri, G. A. Calin, and M. Ivan, "A microRNA component of the hypoxic response," *Cell Death Differ.*, vol. 15, no. 4, pp. 667–671, Apr. 2008.

[6] J. Wang, J. Chen, and S. Sen, "MicroRNA as Biomarkers and Diagnostics," *J. Cell. Physiol.*, vol. 231, no. 1, pp. 25–30, 2016.

[7] L. He *et al.*, "A microRNA component of the p53 tumour suppressor network," *Nature*, vol. 447, no. 7148, pp. 1130–1134, 2007.

[8] J. Ye, M. Xu, X. Tian, S. Cai, S. Zeng, "Research advances in the

detection of miRNA", *J. Pharm. Anal.*, vol. 9, no. 4, pp. 217-226, 2019. doi: 10.1016/j.jpha.2019.05.004.
[9] Y. Cheng, L. Dong, J. Zhang, Y. Zhao, Z. Li, "Recent advances in microRNA detection", *Analyst,* vol. 143, pp. 1758-774, 2018. doi: 10.1039/C7AN02001E.
[10] S. Abasi, S. Minaei, B. Jamshidi, and D. Fathi, "Development of an Optical Smart Portable Instrument for Fruit Quality Detection," *IEEE Trans. Instrum. Meas.*, vol. 70, pp. 1–9, 2021.
[11] A. Gałuszka, Z. M. Migaszewski, and J. Namieśnik, "Moving your laboratories to the field – Advantages and limitations of the use of field portable instruments in environmental sample analysis," *Environ. Res.*, vol. 140, pp. 593–603, Jul. 2015.
[12] M. D. Fernández-Ramos, F. Moreno-puche, P. Escobedo, and P. A. García-lópez, "Optical portable instrument for the determination of CO2 in indoor environments," *Talanta*, vol. 208, no. June 2019, p. 120387, 2020.
[13] Y. Kostov, G. Rao, "Low-cost optical instrumentation for biomedical measurements", Rev. Sci. Instrum., 71, pp. 4361-4374, 2000.
[14] I. Sánchez-Barragán, J.M. Costa-Fernández, A.Sanz-Medel, M. Valledor, F.J. Ferrero, J.C. Campo, "A ratiometric approach for pH optosensing with a single fluorophore indicator", Analytica Chimica Acta, vol. 562, Issue 2, 15, pp. 197-203, 2006.
[15] H.M. Rowe, S.P. Chan, J.N. Demas, B.A. DeGraff, "Self-referencing intensity measurements based on square-wave gated phase-modulation fluorimetry", *Applied Spectroscopy* 57, 532–537, 2003.
[16] G. Liebsch, I. Klimant, C. Krause, O.S.Wolfbeis, "Fluorescent imaging of pH with optical sensors using time-domain dual lifetime referencing", *Analytical Chemistry* 73, 4354–4363. 2001.
[17] M. Valledor, J.C. Campo, F.J. Ferrero, I. Sánchez-Barragán, J.M. Costa-Fernández, A. Sanz-Medel, "A critical comparison between two different ratiometric techniques for optical luminescence sensing", *Sensors and Actuators B: Chemical*, vol. 139, 237–244, 2009.
[18] V. Amendola, R. Pilot, M. Frasconi, O. M Maragò, M. A. Iatì. "Surface plasmon resonance in gold nanoparticles: a review". *Journal of Physics: Condensed Matter*, vol. 29, no. 20, 203002. https://doi.org/10.1088/1361-648X/aa60f3.
[19] P. Eaton, G. Doria, E. Pereira, P. V. Baptista and R. Franco, "Imaging Gold Nanoparticles for DNA Sequence Recognition in Biomedical Applications," in *IEEE Transactions on NanoBioscience*, vol. 6, no. 4, pp. 282-288, Dec. 2007, doi: 10.1109/TNB.2007.908985.
[20] A. Sánchez-Visedo *et al.*, "Visual detection of microRNA146a by using RNA-functionalized gold nanoparticles," *Microchim. Acta*, vol. 187, no. 3, p. 192, Mar. 2020.
[21] Z. Li *et al.*, "Molecular cloning, characterization and expression of miR-15a-3p and miR-15b-3p in dairy cattle," *Mol. Cell. Probes*, vol. 28, no. 5–6, pp. 255–258, 2014.
[22] M. De Planell-Saguer and M. C. Rodicio, "Analytical aspects of microRNA in diagnostics: A review," *Anal. Chim. Acta*, vol. 699, no. 2, pp. 134–152, 2011.
[23] J. L. Matias *et al.*, "Handheld Device for Rapid Detection of miRNA based on a Ratiometric Transmittance Scheme," in *2020 IEEE International Instrumentation and Measurement Technology Conference (I2MTC)*, 2020, pp. 1–4.
[24] R. Elghanian, J. J. Storhoff, R. C. Mucic, R. L. Letsinger, C. A. Mirkin, "Selective Colorimetric Detection of Polynucleotides Based on the Distance-Dependent Optical Properties of Gold Nanoparticles", Science, vol. 277, No. 5329, pp. 1078-1081, 1997. DOI: 10.1126/science.277.5329.1078].
[25] J. Kimling, M. Maier, B. Okenve, V. Kotaidis, H. Ballot, and A. Plech, "Turkevich Method for Gold Nanoparticle Synthesis Revisited," *J. Phys. Chem. B*, vol. 110, no. 32, pp. 15700–15707, Aug. 2006.
[26] LT 1102. Analog Devices. High Speed, Precision, JFET Input Instrumentation Amplifier.
[27] L. Orozco, "Use Synchronous Detection to Make Precision, Low Level Measurments (MS-2698)," *Analog Devices Tech. Artic.*, pp. 1–8, 2014.
[28] L. Orozco, "Optimizing Precision Photodiode Sensor Circuit Design (MS-2624)," *Analog Devices Tech. Artic.*, pp. 1–5, 2014.
[29] IUPAC. Compendium of Chemical Terminology, 2nd ed. (the "Gold Book"). Compiled by A. D. McNaught and A. Wilkinson. Blackwell Scientific Publications, Oxford (1997). Online version (2019-) created by S. J. Chalk. ISBN 0-9678550-9-8. https://doi.org/10.1351/goldbook.
[30] J. Sun, X. Sun, "Recent advances in the construction of DNA nanostructure with signal amplification and ratiometric response for miRNA sensing and imaging", TrAC Trends in Analytical Chemistry, vol. 127, 2020, https://doi.org/10.1016/j.trac.2020.115900.

Adrián Sánchez Visedo was born in Madrid, Spain, in 1989. He received the B.S. degree in Environmental Sciences at Rey Juan Carlos University, Madrid, Spain, and a M.S. degree in Analytical and Bioanalytical Sciences at the University of Oviedo, Oviedo, Spain, in 2015 and 2016 respectively, where he is currently pursuing the Ph.D. degree in Chemical, Biochemical and Structural Analysis and Computational Modeling. He is currently a Ph.D. Student in the Analytical and Bioanalytical Spectrometry Group at University of Oviedo.

Jorge Losada Matías obtained his degree in electronic engineering, and a M.S. in Internet of Things at the University of Oviedo. After doing research at the Gijon Polytechnic School of Engineering, he is currently working as software development engineer at VDI (Value, Development & Innovation).

Ana Soldado Cabezuelo obtained her Ph D. in Chemistry from the University of Oviedo in 2000, currently develops her teaching and scientific activity in the Department of Physical and Analytical Chemistry of the University of Oviedo as an Assistant Professor. From 2001 to 2019 her research work has been carried out in the Regional Institute for Research and Agri-Food Development (SERIDA) of the Principality of Asturias. Her research topic was focused on the development of on-site and real time methodologies for quality and safety control in food and feed, using spectroscopy combined with chemometrics as reference techniques. Some results of the research activity include the supervision of 3 Ph.D. Thesis, author or co-author of 50 articles in indexed in JCR plus 2 book chapters.

José Manuel Costa Fernández is Full Professor at the Department of Physical and Analytical Chemistry and coordinates the Analytical and Bioanalytical Spectrometry research group at Oviedo University (Spain). After obtaining his Ph.D., he was a postdoctoral researcher at the Department of Chemistry, Indiana University (USA). To date, he has supervised 14 Ph.D., is author of more than 145 scientific publications as well as 2 patents related with the development of scientific instrumentation and has presented personally more than 30 invited lectures in International Scientific Conferences. His actual research is focused on the synthesis, characterization, and analytical application of novel photoluminescent nanoparticles.

María Teresa Fernández Argüelles is an Associate Professor at the Department of Physical and Analytical Chemistry (University of Oviedo, Spain), and belongs to the Analytical and Bioanalytical Spectrometry research group. After obtaining her Ph.D., she was postdoctoral researcher at the University of Toronto (Canada), University of East Anglia (UK), and at the International Iberian Nanotechnology Laboratory (Portugal), where she achieved a high degree of specialization in Nanoscience and Bioanalytical Chemistry. Her research interests are the synthesis, surface modification and application of nanoparticles for bioanalytical applications (detection of bacteria, toxins, anions, imaging, etc.).

Marta Valledor Llopis received her M.S. degree in Naval Radio electronics from the University of Cádiz in 1992. In 2006, she received her Ph.D. from the Department of Electrical and Electronic Engineering, University of Oviedo, where she is currently an Associate Professor. Her research interests include electronic instrumentation and measurement (mainly focused on application of photoluminescent techniques based on nanomaterials), fiber-optic sensors, biosensors, biological monitoring, virtual instrumentation, and digital signal processing.

Juan Carlos Campo Rodríguez received his M.S. degree in electrical engineering from the University of Oviedo in 1995 and his Ph.D. degree in 2000. In 1995, he joined the Department of Electrical and Electronic Engineering, University of Oviedo, where he is currently Full Professor and Head of the Gijon Polytechnic School of Engineering. His current research interests include electronic instrumentation and measurement, fiber optic sensors and signal processing.

Francisco Javier Ferrero Martín received the M.S. degree in electrical engineering from the University of Oviedo in 1988 and the Ph.D. in 1998. In 1990, he joined the Department of Electrical and Electronic Engineering, University of Oviedo, where he is currently a Full Professor. His main fields of interest include the development of instrumental systems for measuring chemical, physical and biological variables, based on optical and electrochemical sensors. He is also involved in bioinstrumentation applications for disabled people.